On the Performance of Multi-Stream Receive Spatial Modulation in the MIMO Broadcast Channel

On the Performance of Multi-Stream Receive Spatial Modulation in the MIMO Broadcast Channel

Athanasios Stavridis[(1)], Marco Di Renzo[(2)], and Harald Haas[(1)]
[(1)]Li-Fi Research and Development Centre, Institute for Digital Communications (IDCOM),
School of Engineering, The University of Edinburgh, Edinburgh, UK
[(2)] Paris-Saclay University, Laboratory of Signals and Systems (UMR-8506),
CNRS - CentraleSupelec - University Paris-Sud XI, Paris, France
E–Mail: {a.stavridis, h.haas}@ed.ac.uk, marco.direnzo@lss.supelec.fr

***Abstract*—In this paper, a novel architecture for the Multiple-Input Multiple-Output (MIMO) broadcast channel is proposed and studied. The new architecture is based on the concept of Multi-Stream Receive-Spatial Modulation (MSR-SM). MSR-SM is a closed-loop transmission scheme, which applies the concept of multi-stream space modulation at the receiver side. A new and accurate framework for computing the Average Bit Error Probability (ABEP) of the new architecture is proposed. In addition, the new architecture is compared against the state-of-the-art MIMO transmission in the broadcast channel and it is shown to: i) provide superior Bit Error Rate (BER) performance in the high Signal-to-Noise-Ratio (SNR) regime and ii) reduce the signal processing complexity at the transmitter.**

I. Introduction

A Multiple-Input Multiple-Output (MIMO) communication scheme that has the potential to provide a low complexity system implementation is Spatial Modulation (SM) [1–7]. The operating principle of SM is designed in such a way that the transmitter requires only one Radio Frequency (RF) chain. Therefore, significant Energy Efficiency (EE) and complexity gains are obtained in comparison to conventional MIMO techniques [8]. Due to the potential of SM, several variants of SM have been published [9–11]. A comprehensive overview of the existing literature on SM is given in [6].

As demonstrated in [6], the study of SM and its variants in point-to-point communication is extensive. In addition, the formation of a Multi-User (MU) system based on the concept of SM can be undertaken with the aid of a multiple access scheme, such as Time Division Multiple Access (TDMA), Frequency Division Multiple Access (FDMA), or Orthogonal Frequency-Division Multiple Access (OFDMA). However, a new trend in wireless communication promotes the aggressive allocation of multiple users in the same time and frequency resources. In such systems, usually, the inherent interference is eliminated or mitigated via the deployment of Space Division Multiple Access (SDMA) techniques. In particular, the Multiple Access Channel (MAC) is formed in the uplink [12, 13] and the broadcast channel is established in the downlink [14].

Relevant to this field, [15–18] extend the concept of SM in a MU setup. In particular, the schemes proposed in [15, 16] are applicable to the uplink, whereas the scheme in [17, 18] is suitable for the downlink. Unfortunately, in [15, 16], either there is an increase in the the complexity of the receiver, or there is an error saturation in the Bit Error Rate (BER) performance. In addition, the scheme in [17, 18] has a BER performance degradation with respect to the Single-User (SU) communication. Note that the incorporation of SM in the broadcast channel is a challenging task since the deployment of interference elimination or reduction techniques is difficult. This challenge originates from the way in which information is transmitted in SM. Thus, the design of a SM-based architecture for the broadcast channel becomes a challenging and important task.

Against this background and based on the concept of Multi-Stream Receive-Spatial Modulation (MSR-SM), this paper proposes and studies a new MU architecture for the downlink. MSR-SM is a closed loop and point-to-point modulation scheme which applies the concept of Multi-Stream Spatial Modulation (MS-SM) at the receiver side [19–24]. In more detail, this paper incorporates MSR-SM in the MIMO broadcast channel. This is achieved using Zero Forcing (ZF) forcing precoding.

It is demonstrated that the new architectures outperforms the corresponding conventional spatially multiplexed MIMO broadcast channel, in terms of BER, in high Signal-to-Noise Ratio (SNR). In addition, this paper derives tight upper bounds for the theoretical Average Bit Error Probability (ABEP) of a typical user when: i) the wireless channel follows a Rayleigh distribution and ii) Perfect-Channel State Information at the Transmitter (P-CSIT) is available. This is undertaken by considering an accurate statistical framework for the received signal. The theoretical ABEP of point-to-point MSR-SM has been recently studied in [19, 20]. However, it is emphasized that the mathematical framework derived in this paper exhibits major differences with respect to those presented in [19, 20]. In [19], the statistical description of the received signal is not taken into account. Furthermore, the ABEP computed in [20] is derived for a scenario where a suboptimal detector, which decouples the detection process, is deployed. In contrast, the analysis given in this paper is different for the following reasons: i) multiple users are considered; ii) the statistical description of the received signal of a typical user is considered; and iii) the detection process is based on the Maximum Likelihood (ML) principle, which, as shown in Section IV, imposes some additional mathematical difficulty. Note that the new framework is directly applicable to a point-to-point single

user scenario.

The rest of the paper is organized as follows: The system model of the new architecture is introduced in Section II. The computational complexity of the new architecture is discussed in Section III. The theoretical analysis of the ABEP of a typical user is presented in Section IV. The proposed MU MSR-SM architecture is compared against the corresponding benchmark system in Section V. In addition, numerical results that validate the new theoretical findings are presented in the same section. Finally, the concluding comments of this paper are given in Section VI.

Notation: In the following, lowercase bold letters denote vectors and uppercase bolt letters denote matrices. $(\cdot)^T$, $(\cdot)^H$, tr$(\cdot)$ and $\mathbf{A}^{1/2}$ denote transpose, Hermitian transpose, matrix trace and the square root of $\mathbf{A}$, respectively. $\|\cdot\|_2$ represents the Euclidean norm. $\mathbf{diag}\left(a_1,\ldots,a_n\right)$ represents a diagonal matrix whose main diagonal includes the elements $a_1,\cdots,a_n$. E$[\cdot]$ is the mean value of a RV. A complex Gaussian distribution with mean m and variance σ_C^2 is represented as $\mathcal{CN}(m,\sigma_C^2)$, where its real and imaginary part are independent and identically distributed (i.i.d.) Gaussian RV with distribution $\mathcal{N}(m,\frac{\sigma_C^2}{2})$. Re$\{\cdot\}$ denotes the real part of a complex number or matrix.

II. System Model

In this section, a single cell uncoded downlink transmission is considered. More specifically, a Base Station (BS) with N_t antennas aims to establish the MIMO broadcast channel in order to serve N_u users. Each user is equipped with N_r antennas. Since the transmitter is a BS, the assumption that $N_t \geq N_uN_r$ is realistic. However, if this assumption is not satisfied, user scheduling can be applied in order to overcome this constraint. Furthermore, the MIMO wireless channel between the transmitter and the remote users is assumed to be frequency flat and quasi-static. Finally, in this paper, a scenario where the transmitter possesses P-CSIT, using either the channel reciprocity or fast and error free links from the users, is considered[1].

Due to the availability of P-CSIT, linear precoding can be applied at the transmitter. In addition, the N_t transmit antennas and the $B = N_uN_r$ receive antennas can be interpreted as a $N_t \times B$ MIMO system. In this case, the matrix form of the system equation is given as:

$$\mathbf{y} = \mathbf{HPDx} + \mathbf{w}, \tag{1}$$

where, $\mathbf{y}$ is a $N_uN_r \times 1$ vector which is written as:

$$\mathbf{y} = \left[\mathbf{y}_1^T,\ldots,\mathbf{y}_{N_u}^T\right]^T. \tag{2}$$

Here, $\mathbf{y}_i$, $i = 1,\ldots,N_u$, is the $N_r \times 1$ received signal vector at the i-th user. In addition, the $N_uN_r \times N_t$ wireless channel is denoted as:

$$\mathbf{H} = \left[\mathbf{H}_1^H,\ldots,\mathbf{H}_{N_u}^H\right]^H, \tag{3}$$

[1]Note that supplying the transmitter with P-CSIT is difficult task. Usually, the transmitter is supplied with Imperfect-Channel State Information at the Transmitter (I-CSIT). However, the study of the effect of I-CSIT is out of the scope of this paper.

where, the sub-matrix $\mathbf{H}_i$, $i = 1,\ldots,N_u$, denotes the channel from the transmitter to the i-th user. Furthermore, due to rich scattering, no channel correlation is assumed. In this paper, large scale fading is not considered. Therefore, it is assumed that each sub-matrix $\mathbf{H}_i$ is distributed as $\mathbf{H}_i \sim \mathcal{CN}(\mathbf{0},\mathbf{I})$. In (1),

$$\mathbf{P} = \left[\mathbf{P}_1,\ldots,\mathbf{P}_{N_u}\right] \tag{4}$$

denotes the $N_t \times N_uN_r$ linear precoding matrix. Here, $\mathbf{P}_i$, $i = 1,\ldots,N_u$, is the corresponding precoding matrix for the i-th user. In order to enforce a constrained power transmission, a diagonal normalization matrix:

$$\mathbf{D} = \mathbf{diag}\left(d_1,\ldots,d_{N_uN_r}\right) \tag{5}$$

is deployed. Here, each element d_i, $i = 1,\ldots,N_uN_r$, of the main diagonal of $\mathbf{D}$ equals to:

$$d_i = \sqrt{\frac{1}{\|\mathbf{p}_i\|_2^2}}, \tag{6}$$

where, $\mathbf{p}_i$ corresponds to the i-th column of $\mathbf{P}$. In this way, every column of the normalized precoding matrix:

$$\mathbf{P}_{\text{norm}} = \mathbf{PD} \tag{7}$$

has unity power. Furthermore, the collective information carrying symbol vector at the transmitter is represented by

$$\mathbf{x} = \left[\mathbf{x}_1^T,\ldots,\mathbf{x}_{N_u}^T\right]^T. \tag{8}$$

Here, $\mathbf{x}_i$, $i = 1,\ldots,N_u$, is the signal vector which carries binary information to the i-the user. Finally, the white Gaussian noise is denoted by:

$$\mathbf{w} = \left[\mathbf{w}_1^T,\ldots,\mathbf{w}_{N_u}^T\right]^T, \tag{9}$$

where, $\mathbf{w} \sim \mathcal{CN}(\mathbf{0},\sigma_{\mathbf{w}}^2\mathbf{I})$. Furthermore, $\mathbf{w}_i$, $i = 1,\ldots,N_u$, is the Gaussian noise observed by the i-th user.

In this paper, the linear precoder is designed based on the ZF principle. The selection of ZF precoding is justified by its low complexity and its ability to totally eliminate the interference between different users and between different antennas of the same user. Therefore, ZF precoding can be considered as an efficient method for the formation of a MU architecture based on MSR-SM.

Given that the ZF precoder is the pseudo-inverse of the channel matrix $\mathbf{H}$, its matrix form is written as:

$$\mathbf{P} = \mathbf{H}^H\left(\mathbf{HH}^H\right)^{-1}. \tag{10}$$

In this case, the i-th element of the main diagonal of $\mathbf{D}$ equals to:

$$d_i = \sqrt{\frac{1}{\left[\left(\mathbf{HH}^H\right)^{-1}\right]_{i,i}}},\ i = 1,\ldots,N_uN_r. \tag{11}$$

The incorporation of (10) in (1) gives:

$$\mathbf{y} = \mathbf{Dx} + \mathbf{w}. \tag{12}$$

In addition, the received signal at the i-th is given as:

$$\mathbf{y}_i = \mathbf{D}_i\mathbf{x}_i + \mathbf{w}_i,\quad i = 1,\ldots,N_u. \tag{13}$$

$$\mathbf{x}_i = \left[0,\ldots,0, \underbrace{s_1}_{i_1\text{-th position}}, 0,\ldots,0, \underbrace{s_i}_{i_k\text{-th position}}, 0,\ldots,0, \underbrace{s_{N_s}}_{i_{N_s}\text{-th position}} 0\ldots,0 \right]^T \tag{14}$$

In (13), $\mathbf{D}_i$, $i = 1,\ldots,N_u$, is the $N_r \times N_r$ diagonal normalization matrix of the corresponding precoding matrix $\mathbf{P}_i$. In particular, the normalization matrix $\mathbf{D}$ can be interpreted as the following block diagonal matrix, $\mathbf{D} = \mathbf{diag}\left(\mathbf{D}_1,\ldots,\mathbf{D}_{N_u}\right)$.

From (13), it can be inferred that the structure of $\mathbf{x}_i$, $i = 1,\ldots,N_u$, determines the way that information is transmitted to each user. For example, conventional Spatial MultipleXing (SMX) MIMO transmission is established if all of the elements of $\mathbf{x}_i$ are drawn from a conventional M-ary constellation diagram $\mathcal{M}$.

In order to establish a MSR-SM transmission mechanism between the transmitter and the i-th user, every symbol period, the following two requirements have to be fulfilled. Firstly, $N_s \leq N_r$ conventional symbols have to conveyed from the transmitter to the the i-th user per symbol period. In this way, only a subset of N_s antennas at the i-th user receive a non-zero signal. All of the other antennas face only thermal noise. And secondly, additional binary information has to be encoded via the indices of the N_s (out of N_r) receiving antennas. Note that when $N_s = N_r$, MSR-SM reduces to conventional SMX transmission and no additional information is conveyed via the indices of the receiving antennas.

Provided that the deployed precoding method is ZF, the received signal at each user is given in (13). Hence, via the appropriate selection of the structure of $\mathbf{x}_i$, the transmitter is able to impose that the noise-free received signal $\mathbf{D}_i\mathbf{x}_i$ has exactly N_s non-zero elements and $N_r - N_s$ zero elements. Therefore, the non-zero elements of $\mathbf{D}_i\mathbf{x}_i$ is a scaled version of the corresponding non-zero elements of $\mathbf{x}_i$. Also, the positions of the zero elements of $\mathbf{D}_i\mathbf{x}_i$ are the same as the positions of the zero elements of $\mathbf{x}_i$. Thus, a number of bits can be encoded on the positions of the non-zero elements of $\mathbf{x}_i$.

The structure of the transmission alphabet of MSR-SM, $\mathcal{B}_i$, is given in (14) at the top of this page. As shown in (14), $\mathbf{x}_i \in \mathcal{B}_i$ has exactly N_s non-zero elements which belong to a conventional constellation, $\{s_1,\ldots,s_{N_s}\} \in \mathcal{M}$. Here, $\mathcal{M}$ denotes the deployed constellation. The positions of the non-zero elements of $\mathbf{x}_i$ correspond to the indices of the signal receiving antennas, while the zero elements of $\mathbf{x}_i$ correspond to the indices of the non-receiving antennas. Given that the length of $\mathbf{x}_i$ is N_r and there are N_s non zero elements, the number of total combinations of N_s non-zero elements (receiving antennas) out of N_r is $\binom{N_r}{N_s}$. Here, $\binom{\cdot}{\cdot}$ denotes the binomial coefficient. However, only $k_c = 2^{\log_2\left(\lfloor\binom{N_r}{N_s}\rfloor\right)}$ combinations are used in order to encode $k_2^{\text{MSR-SM}} = \log_2\left(\lfloor\binom{N_r}{N_s}\rfloor\right)$ bits. Also, here, $\lfloor\cdot\rfloor$ denotes the floor function which corresponds a real number to its largest previous integer number. This is done by assigning a unique binary index of length of $k_2^{\text{MSR-SM}}$ bits to each one of the k_c used (legal) combinations. The selection of these (legal) combinations of receiving antennas can be done intelligently in order to minimize the instantaneous BER or it can be done randomly. In the first case, the system complexity is increased and the selection is undertaken adaptively. Given that MSR-SM is a closed loop scheme, the latter case is expected to offer a good performance with no further complexity overhead. In this paper, the focus is on the latter case.

In this way, every symbol period, the bit-stream to be transmitted is divided in two parts. The first part of $k_1^{\text{MSR-SM}} = N_s\log_2(M)$ bits, is encoded and transmitted via N_s symbols drawn from the M-ary constellation $\mathcal{M}$. The second part of $k_2^{\text{MSR-SM}} = \log_2\left(\lfloor\binom{N_r}{N_s}\rfloor\right)$ bits is encoded on the combination of the signal receiving antennas. Therefore, the spectral efficiency of MSR-SM is:

$$k_{\text{MSR-SM}} = N_s\log_2(M) + \log_2\left(\lfloor\binom{N_r}{N_s}\rfloor\right) \tag{15}$$

bits per channel use (bpcu) per user.

Assuming that the i-th user is aware of $\mathbf{D}_i$, the reconstruction of the transmitted bit-streams is conducted by detecting the transmitted vectors $\mathbf{x}_i$, $i = 1,\ldots,N_u$. This is undertaken at every user independently by using the following ML detector:

$$(\tilde{\mathbf{x}}_i) = \arg\min_{\mathbf{x}_i} \|\mathbf{y}_i - \mathbf{D}_i\mathbf{x}_i\|_2^2, \quad i = 1,\ldots,N_u. \tag{16}$$

III. Computation Complexity Analysis

The observation of (14) shows that the sparse structure of the transmission alphabet of MSR-SM, $\mathcal{B}_i$, can be deployed in order to decrease the computational complexity of the transmitter. Assuming that the ZF precoder in (10) is precomputed before the transmission of each block of symbols, the transmitted signal, $\mathbf{s} = \mathbf{PDx}$, in (1) can be calculated with:

$$\mathcal{C}_t = N_t(8N_uN_s - 2) + 2N_uN_s, \tag{17}$$

real operations (additions or multiplications). Hence, lower values of N_s result in lower computational complexity at the transmitter. Note that when it holds that $N_s = N_t$, MSR-SM is transformed into a conventional SMX transmission. In this way, it can be inferred that, at the transmitter side, the computational complexity of MSR-SM is less than the corresponding complexity of conventional SMX transmission.

At the users' side, the ML detection process of the conventional MIMO broadcast channel is decoupled in per single stream detection. Therefore, its detection complexity is lower compared with the corresponding complexity of MU MSR-SM. However, in [20] a suboptimal detector for MSR-SM is proposed. This detector achieves almost the same computational complexity as the previous decoupled detector. The study of the detector of [20] is, however, outside of the scope of this paper.

$$\delta_{k+1} = \begin{cases} 1, & k = -1, \\ \frac{k}{k+1} \sum_{i=1}^{k+1} \left[\sum_{j=1}^{N} \left(1 - \frac{\alpha_1}{\alpha_j} \right)^i \right] \delta_{k+1-i}, & k = 0, 1, 2, \ldots . \end{cases} \quad (24)$$

IV. Theoretical Evaluation of the Average Bit Error Probability

In this section, the ABEP of a typical user is derived. Based on the union bound technique, the ABEP of the i-th user, $P_{\text{bit}}^{i}(\gamma)$, for a given transmit SNR γ, is bounded as:

$$P_{\text{bit}}^{i}(\gamma) \leq \frac{1}{|\mathcal{B}_i| k_{\text{MSR-SM}}} \sum_{\mathbf{x}_i} \sum_{\substack{\hat{\mathbf{x}}_i \\ \hat{\mathbf{x}}_i \neq \mathbf{x}_i}} d(\mathbf{x}_i \rightarrow \hat{\mathbf{x}}_i) P_{\text{e}}^{i}(\mathbf{x}_i \rightarrow \hat{\mathbf{x}}_i, \gamma). \quad (18)$$

In (18), $P_{\text{e}}^{i}(\mathbf{x}_i \rightarrow \hat{\mathbf{x}}_i, \gamma)$ denotes the Pairwise Error Probability (PEP) of transmitting $\mathbf{x}_i$ to the i-th user while its detector erroneously decides in favor of $\hat{\mathbf{x}}_i$. The Hamming distance between the bit-words represented by $\mathbf{x}_i$ and $\hat{\mathbf{x}}_i$ is denoted as $d(\mathbf{x}_i \rightarrow \hat{\mathbf{x}}_i)$. Also, the size of the transmission alphabet of MSR-SM to the i-th user is given as $|\mathcal{B}_i| = M^{N_s} 2^{\left\lfloor \log_2 \binom{N_r}{N_s} \right\rfloor}$.

The evaluation of (18) requires the knowledge of $P_{\text{e}}^{i}(\mathbf{x}_i \rightarrow \hat{\mathbf{x}}_i, \gamma)$, which is the expectation of the instantaneous PEP over all channel realizations. The instantaneous PEP of the i-th user is expressed as:

$$P_{\text{e}}^{i}\left(\mathbf{x}_i \rightarrow \hat{\mathbf{x}}_i, \gamma | \mathbf{D}_i^2\right) = Q\left(\sqrt{\frac{\mathbf{c}_i^H \mathbf{D}_i^2 \mathbf{c}_i}{2} \gamma} \right) = Q\left(\sqrt{\frac{z_i \gamma}{2}} \right), \quad (19)$$

where, $\mathbf{c}_i = \mathbf{x}_i - \hat{\mathbf{x}}_i$; $z_i = \mathbf{c}_i^H \mathbf{D}_i^2 \mathbf{c}_i$; and $\gamma = 1/\sigma_{\mathbf{w}_i}^2$ is the transmit SNR. The proof of (19) relies on the fact that a symbol error occurs at the i-th user when, $\mathcal{E}_i\left(\mathbf{x}_i, \hat{\mathbf{x}}_i\right) = \left\{ \|\mathbf{y}_i - \mathbf{D}_i \mathbf{x}_i\|_2^2 > \|\mathbf{y}_i - \mathbf{D}_i \hat{\mathbf{x}}_i\|_2^2 \right\}$. It is not difficult to show that, $\mathcal{E}_i\left(\mathbf{x}_i, \hat{\mathbf{x}}_i\right) = \left\{ -\text{Re}\{\mathbf{c}_i^H \mathbf{D}_i \mathbf{w}_i\} > \frac{\mathbf{c}_i^H \mathbf{D}_i^2 \mathbf{c}_i}{2} \right\}$. Therefore, using the statistical distribution of $\mathbf{w}_i$, the PEP of the i-th user is expressed as in (19).

The observation of the instantaneous PEP of the i-th user in (19) shows that it is conditioned on the Random Variable (RV) z_i. Thus, the Probability Density Function (PDF) of z_i has to be derived. However, it holds that:

$$z_i = \sum_{k=1}^{N_r} |x_k - \hat{x}_k|^2 d_k^2 = \sum_{x_k - \hat{x}_k \neq 0} |x_k - \hat{x}_k|^2 d_k^2. \quad (20)$$

In [25], it is explicitly shown that d_k is a gamma RV with $d_k^2 \sim \text{Gamma}\left(L_{\text{MU}}, 1\right)$, where, $L_{\text{MU}} = N_t - N_u N_r + 1$. Therefore, the RV $Z_k = |x_k - \hat{x}_k|^2 d_k^2$ is also a gamma RV, when it holds that $x_k - \hat{x}_k \neq 0$. Here, for notational convenience, the following variable is introduced, $b_k = |x_k - \hat{x}_k|^2$. Based on the previous arguments, the PDF of Z_k is given as:

$$f_{Z_k}(x) = \frac{1}{b_k^L \Gamma(L)} x^{L-1} e^{\frac{x}{b_k}} H_0(x), \quad (21)$$

where, $H_0(x)$ is the Heaviside step function, for which it holds that: $H_0(x) = 0$ for $x < 0$ and $H_0(x) = 1$ for $x \geq 0$.

Usually, in published research, the RVs d_k^2 are assumed to be statistically independent in order to simplify the whole analysis [26]. This assumption is in contradiction with the structure of $d_k^2 = 1/\left[\left(\mathbf{H}_i \mathbf{H}_i^H \right)^{-1} \right]_{k,k}$, since the realization of every RV d_k^2 occurs using the same mathematical operation on the same random matrix $\mathbf{H}_i$.

In this paper, the statistical dependence of the RVs d_k^2 is considered. For this reason, z_i is the result of the sum of correlated gamma RVs. Thus, using the result from [27, Corollary 1] and (20), the PDF of z_i is directly expressed as:

$$f_{z_i}(x) = \left[\prod_{l=1}^{N_i} \left(\frac{\alpha_1}{\alpha_l} \right)^L \right] \left[\sum_{k=0}^{+\infty} \frac{\delta_k x^{N_i L + k - 1} e^{-\frac{x}{\alpha_1}}}{\alpha_1^{N_i L + k} \Gamma\left(N_i + k\right)} \right] H_0(x), \quad (22)$$

where, N_i is the number of non zero elements of $\mathbf{c}_i$ for a given pair of $\mathbf{x}_i$ and $\hat{\mathbf{x}}_i$. In (22), α_l, $l = 1, \ldots, N_i$, denote the eigenvalues of $\mathbf{A} = \mathbf{BR}$ in ascending order. Here, $\mathbf{B}$ is defined as the following diagonal matrix, $\mathbf{B} = \mathbf{diag}\left(b_1, \ldots, b_{N_i}\right)$, where, b_l, $l = 1, \ldots, N_i$, is the absolute value of the l-th non zero element of $\mathbf{c}_i$. Also, $\mathbf{R}$ is a $N_i \times N_i$ matrix defined as:

$$\mathbf{R} = \begin{bmatrix} 1 & \sqrt{\rho_c} & \cdots & \sqrt{\rho_c} \\ \sqrt{\rho_c} & \ddots & \ddots & \vdots \\ \vdots & \ddots & \ddots & \sqrt{\rho_c} \\ \sqrt{\rho_c} & \cdots & \sqrt{\rho_c} & 1 \end{bmatrix}, \quad (23)$$

where, ρ_c is the Pearson product-moment correlation coefficient between any pair of two different RVs of the main diagonal of $\mathbf{D}_i^2$. Finally, δ_k, $k = 0, 1, 2, \ldots$, are given in (24) at the top of this page.

In order to further simplify (19), the Chernoff bound of the Q-function, $Q\left(x\right) \leq \frac{1}{2} e^{-\frac{x^2}{2}}$, is considered. In this way, the PEP of the i-th user is expressed as:

$$\begin{aligned} P_{\text{e}}^{i}\left(\mathbf{x}_i \rightarrow \hat{\mathbf{x}}_i, \gamma_i\right) &\leq \frac{1}{2} \text{E}_{z_i}\left[e^{-\frac{z_i \gamma_i}{4}} \right] \\ &= \frac{1}{2} \int_{-\infty}^{+\infty} e^{-\frac{y \gamma_i}{4}} f_{z_i}(y) \text{d}y. \end{aligned} \quad (25)$$

Provided that the PDF of z_i is given from (22), after some algebraic manipulations which are omitted here due to space limitation, the evaluation of (25) gives:

$$\begin{aligned} P_{\text{e}}^{i}(\mathbf{x}_i \rightarrow \hat{\mathbf{x}}_i, \gamma) \leq & \frac{\left[\prod_{l=1}^{N_i} \left(\frac{\alpha_1}{\alpha_l} \right)^{L_{\text{MU}}} \right]}{2} \left(\frac{\alpha_1}{4} \xi_i \gamma + 1 \right)^{-N_i L_{\text{MU}}} \\ & \times \sum_{k=0}^{+\infty} \delta_k \left(\frac{\alpha_1}{4} \xi_i \gamma + 1 \right)^{-k}. \end{aligned} \quad (26)$$

Therefore, the computation of the ABEP of the i-th user is conducted from (18), by using (26). Note that the derived bounds are directly applicable to the conventional MIMO broadcast channel when $N_s = N_r$.

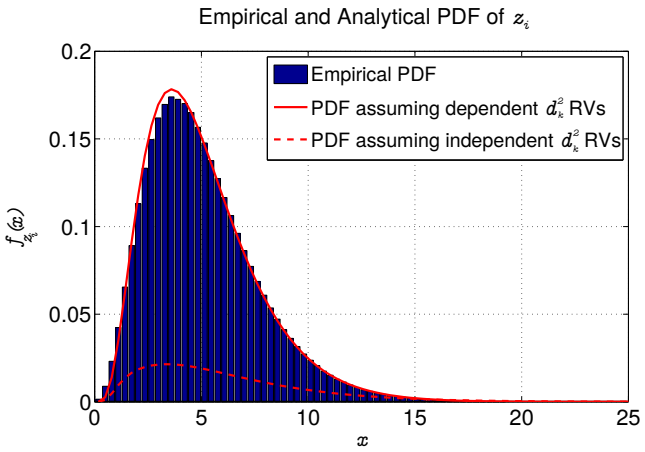

Fig. 1. Illustration of empirical and analytical PDF of (20) by assuming that: i) the RVs d_k, $k = 1, \ldots, 2$ are statistically dependent and ii) they are independent. Setup: $\mathbf{H} \sim \mathcal{CN}(\mathbf{0}_{2\times 4}, \mathbf{I}_{2\times 4})$; and ii) $b_1 = 0.5$ and $b_1 = 1.2$, where, b_i, $i = 1, 2$, are parameters defined in (21).

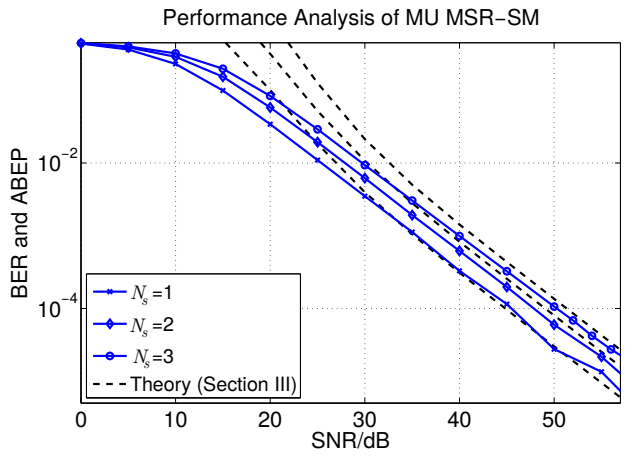

Fig. 2. Performance analysis of a typical user, when MSR-SM is deployed and the precoding method is ZF with P-CSIT: simulation results vs. the bounds in Section IV. Setup: $N_t = 16$, $N_r = 4$, $N_u = 4$, $N_s = \{1, 2, 3\}$, and $M = 4$.

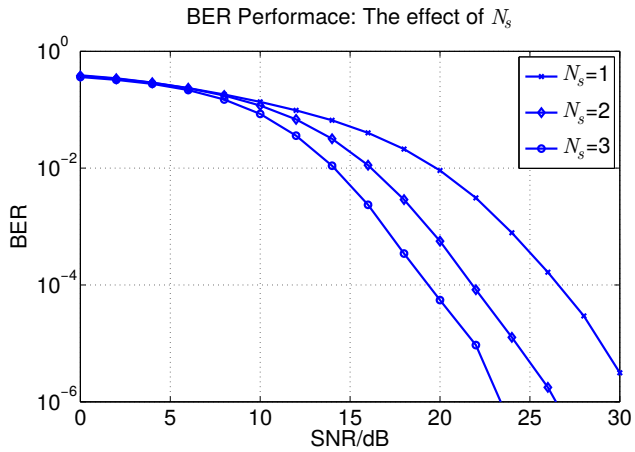

Fig. 3. BER performance of a typical user of MU MSR-SM as a function of N_s. Setup: $N_t = 20$, $N_r = 4$, $N_u = 4$. The spectral efficiency is 8 bpcu.

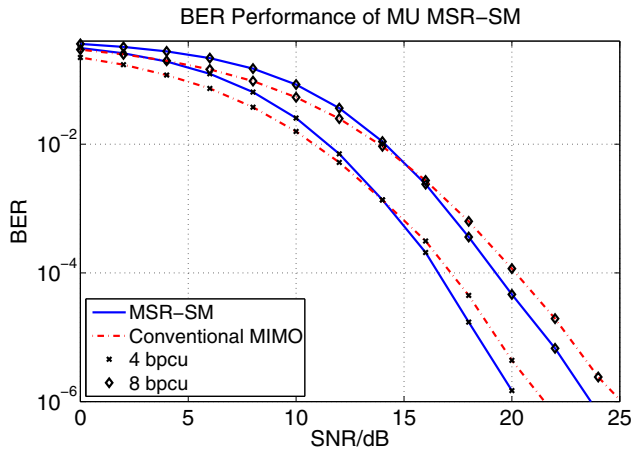

Fig. 4. BER performance of MSR-SM versus the conventional MIMO broadcast channel. Setup: $N_t = 20$, $N_r = 4$, and $N_u = 4$.

V. Simulation Results and Discussion

The main objectives of this section are: i) the validation of the theoretical results of Section IV and ii) the comparison of the new MU architecture with the corresponding State-of-the-Art (SotA) benchmark scheme. In this section, the wireless channel is assumed to follow a Rayleigh distribution.

Section IV provides the derivation of the ABEP of MU MSR-SM using the PDF of z_i given in (22). The deployment of (22) relies on the fact that the RVs d_k^2, $k = 1, \ldots, N_r$, are statistically dependent. In order to confirm that the RVs d_k^2 are statistical dependent, Fig. 1 depicts the empirical PDF of (20) against its analytical form as given in (22). In addition, Fig. 1 presents the analytical PDF of (22) under the assumption that d_k^2, $k = 1, \ldots, N_r$, are statistically independent RVs. If this assumption was valid, the PDF of (20) could be directly obtained using the result from [27, Theorem 1]. From Fig. 1, it can be concluded that the theoretical PDF of (22) perfectly matches its empirical PDF. In contrast, when the RVs d_k^2, $k = 1, \ldots, N_r$ are assumed to be independent, the obtained PDF from [27, Theorem 1] deviates from the empirical results.

As a form of validation of the bounds derived in Section IV, in Fig. 2, these bounds are compared against the corresponding BER curves obtained via Monte Carlo simulations. The observation of Fig. 2 shows that the upper bounds are tight in high SNR regime. In low SNR, there is a gap between the theoretical and simulated curves. However, this gap is a well known effect of the union bound technique deployed in Section IV [28].

In Fig. 3, the BER performance of MU MSR-SM as a function of N_s is shown for the same spectral efficiency. In particular, Fig. 3 demonstrates that the BER of a typical user improves as N_s increases. This happens because higher values of N_s require a lower modulation order of Quadrature Amplitude Modulation (QAM) in order to achieve the same spectral efficiency. However, as shown in Fig 4, the optimal value of N_s is not to N_r, i.e., the conventional MIMO broadcast channel.

A comparison between the BER performance of MU MSR-SM and the corresponding benchmark system is presented in Fig. 4. In this paper, the selected benchmark system is the conventional spatially multiplexed MIMO broadcast channel, where N_r symbol streams are established per user. The spectral efficiency of both schemes is set to be the same by selecting the appropriate constellation order. In addition, MU MSR-SM spatially modulates $N_s = 2$ and $N_s = 3$ parallel symbol streams in order to achieve 4 and 8 bpcu, respectively. As shown in Fig. 4, in low SNR the conventional MIMO broadcast channel offers a slightly better performance than MU MSR-SM. However, for practical values of BER approximately less than 10^{-2}, MU MSR-SM outperforms the benchmark systems. The performance gap between the considered schemes is about 0.5 dB and 1 dB for 4 and 8 bpcu, respectively. Furthermore, Fig. 4 indicates that MU MSR-SM achieves the same diversity order as the benchmark system but higher coding gain. The theoretical proof of the previous indication is a subject of our future work.

VI. Conclusions

The incorporation of MSR-SM in the MIMO broadcast channel was introduced and studied in this paper. In particular, a novel upper bound for the theoretical BER of the new architecture was derived. This was undertaken by using a new and accurate statistical framework for the received signal of a typical user. It was shown that the new bounds are tight. For the purpose of comparison, MU MSR-SM was evaluated, in terms of BER, against the corresponding conventional MIMO broadcast channel. It was shown that the new architecture outperforms the benchmark system in high SNR regime. Also, it offers lower computational complexity in the transmitter. Therefore, MSR-SM could be considered as an alternative transmission mechanism for the MIMO broadcast channel.

Finally, the derivation of the diversity order and coding of MU MSR-SM, as well as its theoretical comparison with the SotA is a subject of our future work.

Acknowledgement

Professor Harald Haas acknowledges support by EPSRC under grant EP/K008757/1.

References

[1] M. Di Renzo, H. Haas, and P. M. Grant, "Spatial modulation for multiple-antenna wireless systems: A survey," *IEEE Commun. Mag.*, vol. 49, no. 12, pp. 182–191, December 2011.

[2] R. Mesleh, H. Haas, S. Sinanović, C. W. Ahn, and S. Yun, "Spatial modulation," *IEEE Trans. on Veh. Tech.*, vol. 57, no. 4, pp. 2228 – 2241, Jul. 2008.

[3] M. Di Renzo and H. Haas, "Bit error probability of SM-MIMO over generalized fading channels," *IEEE Trans. on Vehicular Techn.*, vol. 61, no. 3, pp. 1124–1144, March 2012.

[4] A. Younis, W. Thompson, M. D. Renzo, C.-X. Wang, M. A. Beach, H. Haas, and P. M. Grant, "Performance of spatial modulation using measured real-world channels," in *Proc. of the 78th IEEE Veh. Tech. Conf. (VTC)*, Las Vegas, USA, Sep. 2–5 2013.

[5] N. Serafimovski, A. Younis, R. Mesleh, P. Chambers, M. D. Renzo, C.-X. Wang, P. M. Grant, M. A. Beach, and H. Haas, "Practical implementation of spatial modulation," *IEEE Trans. on Veh. Tech.*, vol. 62, no. 9, pp. 4511–4523, 2013.

[6] M. Di Renzo, H. Haas, A. Ghrayeb, S. Sugiura, and L. Hanzo, "Spatial modulation for generalized MIMO: Challenges, opportunities, and implementation," *Proc. IEEE*, vol. 102, no. 1, pp. 56–103, Jan 2014.

[7] P. Yang, M. Di Renzo, Y. Xiao, S. Li, and L. Hanzo, "Design guidelines for spatial modulation," *IEEE Commun. Surveys Tut.*, vol. 17, no. 1, pp. 6–26, First Quarter 2015.

[8] A. Stavridis, S. Sinanović, M. D. Renzo., and H. Haas, "Energy evaluation of spatial modulation at a multi-antenna base station," in *Proc. of the 78th IEEE Veh. Tech. Conf. (VTC)*, Las Vegas, USA, Sep. 2–5, 2013.

[9] J. Jeganathan, A. Ghrayeb, L. Szczecinski, and A. Ceron, "Space shift keying modulation for MIMO channels," *IEEE Trans. on Wireless Commun.*, vol. 8, no. 7, pp. 3692–3703, Jul. 2009.

[10] M. Wen, X. Cheng, H. Poor, and B. Jiao, "Use of SSK modulation in two-way amplify-and-forward relaying," *IEEE Trans. on Veh. Techn.*, vol. 63, no. 3, pp. 1498–1504, March 2014.

[11] P. Som and A. Chockalingam, "Performance analysis of space-shift keying in decode-and-forward multihop MIMO networks," *IEEE Trans. on Veh. Techn.*, vol. 64, no. 1, pp. 132–146, Jan 2015.

[12] M. Matthaiou, N. Chatzidiamantis, G. Karagiannidis, and J. Nossek, "ZF detectors over correlated K fading MIMO channels," *IEEE Trans. on Commun.*, vol. 59, no. 6, pp. 1591–1603, June 2011.

[13] M. Bhatnagar and A. Hjorungnes, "Improved interference cancellation scheme for two-user detection of Alamouti code," *IEEE Trans. Signal Process.*, vol. 58, no. 8, pp. 4459–4465, Aug 2010.

[14] M. Kountouris and J. Andrews, "Downlink SDMA with limited feedback in interference-limited wireless networks," *IEEE Trans. on Wireless Commun.*, vol. 11, no. 8, pp. 2730–2741, August 2012.

[15] N. Serafimovski, S. Sinanovic, M. Renzo, and H. Haas, "Multiple access spatial modulation," *EURASIP J. on Wireless Commun. and Netw.*, vol. 2012, no. 1, pp. 1–20, 2012.

[16] M. Di Renzo and H. Haas, "Bit error probability of space-shift keying MIMO over multiple-access independent fading channels," *IEEE Trans on Veh. Technol.*, vol. 60, no. 8, pp. 3694–3711, Oct 2011.

[17] S. Narayanan, M. J. Chaudhary, A. Stavridis, R. Di Renzo, F. Graziosi, and H. Haas, "Multi-user spatial modulation MIMO," in *Proc. of IEEE Wireless Communications and Networking Conference (WCNC)*, Apr. 6–9, 2014.

[18] X. Li, Y. Zhang, L. Xiao, X. Xu, and J. Wang, "A novel precoding scheme for downlink multi-user spatial modulation system," in *Proc. IEEE 24th Int. Symp. Pers. Indoor and Mobile Radio Commun. (PIMRC)*, Sept 2013, pp. 1361–1365.

[19] R. Zhang, L.-L. Yang, and L. Hanzo, "Generalised pre-coding aided spatial modulation," *IEEE Trans. on Wireless Commun.*, vol. 12, no. 11, pp. 5434–5443, November 2013.

[20] ——, "Error probability and capacity analysis of generalised pre-coding aided spatial modulation," *IEEE Trans. on Wireless Commun.*, vol. PP, no. 99, pp. 1–1, 2014.

[21] A. Stavridis, D. Basnayaka, S. Sinanovic, M. Di Renzo, and H. Haas, "A virtual MIMO dual-hop architecture based on hybrid spatial modulation," *IEEE Trans. on Commun.*, vol. 62, no. 9, pp. 3161–3179, Sept 2014.

[22] A. Stavridis, D. Basnayaka, M. Di Renzo, and H. Haas, "Average bit error probability of receive-spatial modulation using zero-forcing precoding," in *IEEE 19th Int. Workshop on Computer Aided Modeling and Des. of Commun. Links and Netw. (CAMAD)*, 2014.

[23] J. Wang, S. Jia, and J. Song, "Generalised spatial modulation system with multiple active transmit antennas and low complexity detection scheme," *IEEE Trans. on Wireless Commun.*, vol. 11, no. 4, pp. 1605 – 1615, April 2012.

[24] K. Ntontin, M. Di Renzo, A. Perez-Neira, and C. Verikoukis, "Performance analysis of multistream spatial modulation with maximum-likelihood detection," in *Proc. of 2013 IEEE Global Commun. Conf. (GLOBECOM)*, Dec 2013, pp. 1590–1594.

[25] D. Gore, R. Heath, and A. Paulraj, "Transmit selection in spatial multiplexing systems," *IEEE Commun. Lett.*, vol. 6, no. 11, pp. 491–493, Nov 2002.

[26] C.-J. Chen and L.-C. Wang, "Performance analysis of scheduling in multiuser MIMO systems with zero-forcing receivers," *IEEE J. Sel. Areas Commun.*, vol. 25, no. 7, pp. 1435–1445, September 2007.

[27] M.-S. Alouini, A. Abdi, and M. Kaveh, "Sum of gamma variates and performance of wireless communication systems over Nakagami-fading channels," *IEEE Trans. on Veh. Technol.*, vol. 50, no. 6, pp. 1471–1480, Nov 2001.

[28] J. G. Proakis, *Digital Communications*, 4th ed. New York, NY, USA: McGraw–Hill, 2000.